Princeton Plasma Physics Laboratory

PPPL- 4313

PPPL- 4313

# Cross-Field Current Instabilities in Thin Ionization Layers and the Enhanced Aurora

Jay R. Johnson and Hideo Okuda

May 2008

Prepared for the U.S. Department of Energy under Contract DE-AC02-76CH03073.

# Princeton Plasma Physics Laboratory
# Report Disclaimers

---

## Full Legal Disclaimer



## Trademark Disclaimer



---

# PPPL Report Availability

## Princeton Plasma Physics Laboratory:

http://www.pppl.gov/techreports.cfm

## Office of Scientific and Technical Information (OSTI):

http://www.osti.gov/bridge

---

**Related Links:**

**U.S. Department of Energy**

**Office of Scientific and Technical Information**

**Fusion Links**

to be submitted to *J. Geophys. Res.*, 2008.

# Cross-Field Current Instabilities in Thin Ionization Layers and the Enhanced Aurora

Jay R. Johnson and Hideo Okuda

Princeton University, Plasma Physics Laboratory, Princeton, NJ

**Abstract.** Nearly half of the time, auroral displays exhibit thin, bright layers known as "enhanced aurora." There is a substantial body of evidence that connects these displays with thin, dense, heavy ion layers in the E-region. Based on the spectral characteristics of the enhanced layers, it is believed that they result when wave-particle interaction heats ambient electrons to energies at or just above the 17 eV ionization energy of $N_2$. While there are several possible instabilities that could produce suprathermal electrons in thin layers, there has been no clear theoretical investigation which examines in detail how wave instabilities in the thin ionization layers could develop and produce the suprathermal electrons. We examine instabilities which would occur in thin, dense, heavy ion layers using extensive analytical analysis combined with particle simulations. We analyze a cross field current instability that is found to be strongly unstable in the heavy ion layers. Electrostatic simulations show that substantial heating of the ambient electrons occurs with energization at or above the $N_2$ ionization energy.

## 1. Introduction

### 1.1. Enhanced Aurora

The luminosity in visible auroral forms is typically distributed vertically over an altitude range of several tens to hundreds of kilometers [*Störmer*, 1955]. The luminosity profiles normally agree well with calculated profiles for the collisional ionization and excitation by atmospheric particles by precipitating electrons having energies 100eV-10keV. However, auroras frequently (typically more than 50% of the time) exhibit enhanced intensity within relatively thin horizontal layers, and the layers appear to be relatively stable atmospheric structures [*Hallinan et al.*, 1985].

An example of an enhanced aurora is shown in Figure 1 from *Hallinan et al.* [1985]. In the photograph, it is possible to see a thin, bright enhancement in the auroral curtain just above the bottom of the aurora. The enhanced luminous layer remains primarily horizontal. The enhanced layer may also be near the top of the aurora when it is typically called a sharp upper border or near the bottom of the aurora when it is

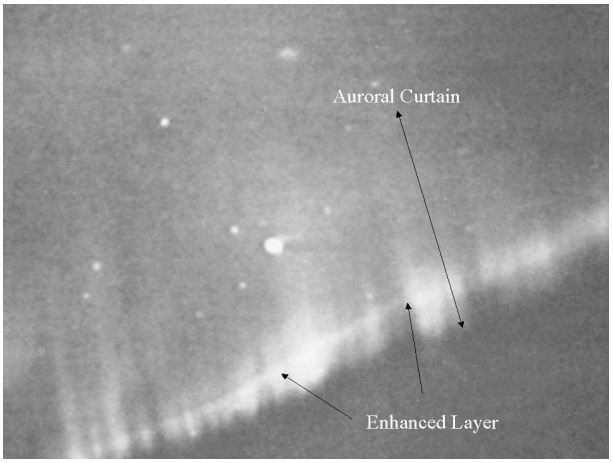


**Figure 1.** An image of an enhanced auroral layer as shown in *Hallinan et al.* [1985].

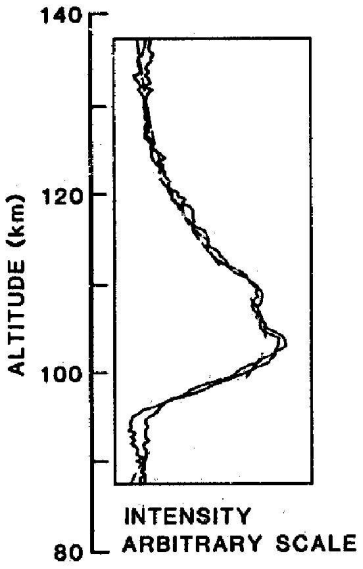


**Figure 2.** A plot of intensity of an auroral arc with two enhanced layers around 105 km and 110 km. The thickness of the layers is a few km.

called an enhanced lower border.

A typical luminosity of an auroral arc with an embedded enhanced layer is shown in Figure 2 from *Hallinan et al.* [1985]. Note that the arc extends from 130 km down to 95 km. Two enhanced layers are seen at altitudes around 105 and 110 km each exhibiting a thickness of a few km.

In general, the enhanced layers most often occur at altitudes ranging from 90 to 130 km. Multiple layers are commonly observed as in Figure 2. Most of the time, the layers have a thickness less than 1 km, but the layers can also be thick—extending from 5-15 km. The thick layers usually have a sharp upper border. Typical luminosity enhancements range up to a factor of 5:1.

The layers appear to be quite stable and may remain in the evening sector for one or two hours. Strong evidence that the layers are related to relatively stable atmospheric structures comes from auroras with high variability. Such active aurorae may have variations in the downcoming electron flux which causes the aurora to suddenly penetrate to lower altitude. When this phenomenon occurs, the location of the enhanced aurora remains the same, but the relative location within the arc changes [*Hallinan et al.*, 1985]. For example, an enhanced lower border may suddenly appear as a luminous layer in the middle

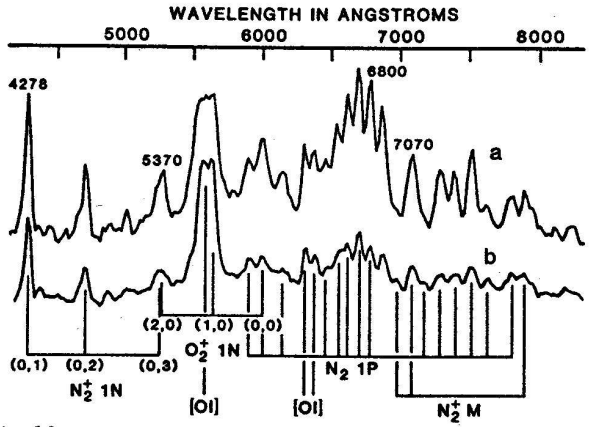


**Figure 3.** The spectra of an enhanced auroral layer and the surrounding arc from *Hallinan et al.* [1985]. Note that enhancements are found uniformly over the entire spectrum including the $N_2^+$ lines which require at least 17 eV electrons.

of the arc. Similarly, when there is a variable arc, the enhanced layer will reappear when precipitation recurs.

The nature of the optical spectra of the enhanced emissions is important because it contains the key to understanding the energization process responsible for the enhanced aurora. In Figure 3 we show the spectrum obtain inside the enhanced layer compared with the spectrum obtained just above the arc [*Hallinan et al.*, 1985]. The most striking feature is that all luminosity bands are enhanced. The fact that the $4278\text{Å}N_2^+$ band is enhanced is significant because it means that the electrons responsible for the emissions must have energies above the ionization energy for $N_2$ (around 17 eV). The observations suggest that the ambient electron population develops an energetic tail which ranges to energies up to 20 eV. It should be noted, however, that the enhancement ratio does increase from blue to red, which suggests that the electron tail may have an upper limit near 20 eV.

On the other hand, the $N_2^+$ emission is sometimes suppressed in an enhanced aurora as seen in the spectrum from an enhanced lower border shown in Figure 4 from *Hallinan et al.* [1997]. In this figure, the following lines are shown: $4709\text{Å}N_2^+$, $5275\text{Å}O_2^+$, $5577\text{Å}O$, $6624\text{Å}N_2$, $6705\text{Å}N_2$, $6789\text{Å}N_2$ and $6874\text{Å}N_2^+$. First, it is to be noted that basically all the bands are enhanced, but that the ionized $4709\text{Å}N_2^+$ and $5275\text{Å}O_2^+$ bands are not as strongly enhanced. This fact suggests that the electrons responsible for the

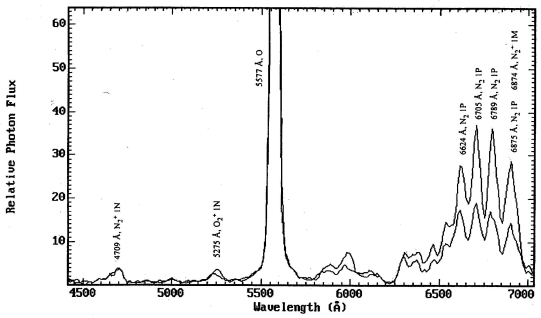


**Figure 4.** A comparison between the spectral emission in a thin enhanced layer and the emission from the arc just above the enhanced layer from *Hallinan et al.* [1997]. In this case, there is enhancement in the neutral $N_2$ lines, but not as much in the ionized line at 4709Å$N_2^+$ indicating that there is a sharp cutoff in the electron energy above 17 eV.

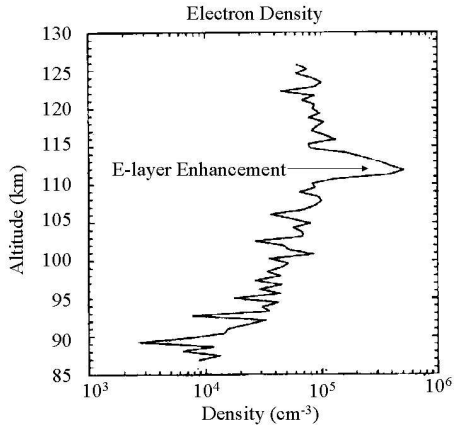


**Figure 5.** The density profile of electrons in in the E-region measured by incoherent-scatter radar during the five minute period 2105-2120 UT on July 27, 1991 [*Bristow et al.*, 1993]. A thin ionization layer can be seen around 110 km. The thin layer remained at this altitude for around 2 hours.

energization have energies sufficient to excite the $N_2$ bands, but insufficient energy to ionize $N_2$ to produce the $N_2^+$ bands. Therefore, in some cases is an enhancement of electrons with energies between 10 eV and 20 eV with a sharp cutoff above 20 eV *Hallinan et al.* [1997].

Two major conclusions may be drawn from these observations. First, the atmosphere in the auroral zone contains one or more very thin layers that may interact with precipitating electrons and or auroral currents. Second, because collisional models for electron precipitation cannot produce such thin layers, it is likely that a collective plasma process may be responsible for energizing the particles in these layers.

### 1.2. Thin Ionization Layers in the Ionosphere

The existence of thin ionization layers in the ionosphere have been known for decades [*Dungey*, 1963; *Whitehead*, 1961; *Axford*, 1963]. The only reasonable explanation for such long-lived layers was the redistribution of background ionization which could occur when there are: (a) appropriately directed shear flows in a neutral gas which can lead to the formation of irregularities and/or (b) strong electric fields that can generate vertical ion velocity profiles with large gradients. Strong electric fields are found in the high latitude ionosphere where the aurora regularly occurs and seems most relevant.

The thin ionization layers in the E-region have been observed at high-latitude by high resolution incoherent-scatter observations. In Figure 5 from *Bristow and Watkins* [1993] we show an example of the electron density showing the presence of a thin layer at about 110 km altitude for data obtained from the incoherent-scatter technique during the five minute period 2105-2120 UT on July 27, 1991. From observations obtained over a longer time period, 2000-2200 UT, it is apparent that the layer remained near the same altitude for a two hour period and the thickness of the ionization layer ranged between 1.5 and 2.5 km while the peak density ranged from $10^5$ to $10^6 \mathrm{cm}^{-3}$.

Plasma may accumulate into such thin layers at high latitude in the presence of ionospheric electric fields [*Nygrén et al.*, 1984b]. The accumulation occurs because the mobility of ions in response to a DC electric field changes character when there are changes in the ratio of the collision frequency to the cyclotron frequency. At high altitudes, the ions move in the $\mathbf{E} \times \mathbf{B}$ direction (Hall mobility) while at lower altitude, the response is in the perpendicular (to $\mathbf{B}$) electric field direction (Pederson mobility). The ions are impeded by neutral collisions and the electrons carry the currents across the magnetic field.

This situation is shown schematically in Figure 6. The dipole field makes a dip angle with respect to the vertical direction, $\theta$. A perpendicular electric field makes an angle $\phi$ with respect to the projection of

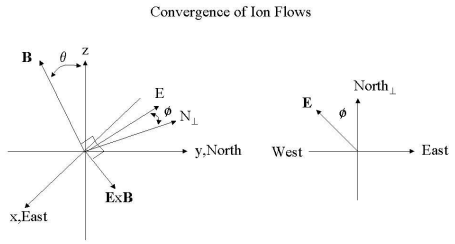


**Figure 6.** Ions can accumulate into thin layers where the Hall and Pederson conductivities have a similar value when the electric field is in the appropriate sector. For the electric field shown, the Hall effects at higher altitude drive the ions downward, while Pederson effects at lower altitudes drive the ions upward.

the northward direction. The equilibrium flow profile is the solution to

$$q(\mathbf{E} + \mathbf{v} \times \mathbf{B}) - m_i \nu_{in}(\mathbf{v} - \mathbf{u}) = 0 \qquad (1)$$

where $\nu_{in}$ is the neutral-ion collision frequency and $\mathbf{u}$ is the neutral velocity. The vertical component of the ion velocity is

$$v_{iz} = \frac{E/B}{1 + b^2}(b\cos\phi - \sin\phi)\cos\theta \qquad (2)$$

where $b \equiv \nu_i/\Omega_i$.

There is a convergent null where $b = \tan\phi$ and the vertical component of the Hall mobility above the null is downward while the vertical component of the Pederson mobility below the null is upward. Such a null can lead to convergent flow into a thin ionization layer.

Normal ionospheric molecules such as $NO^+$ and $O_2^+$ have such high recombination rates that regions of high concentration of plasma density would be prevented [*Nygrén et al.*, 1984b]. The presence of long-lived metallic ions such as $Fe^+$ and $Mg^+$ is a key factor in the formation of thin layers. Metallic ions originate from meteor ablation and exist at low densities over a wide range of altitudes [*Kelley*, 1989]. Because of the long recombination times (hours to days), these ions can accumulate to high densities with limitations from pressure gradient, total metallic ion content and possible wave transport induced by the formation of the layers. Moreover, large concentrations of metal ions have been observed in rocket [*Narcisi et al.*, 1968] and incoherent scatter experiments [*Behnke and Vickrey*, 1975; *Turunen et al.*, 1988]. In Figure 7 we show

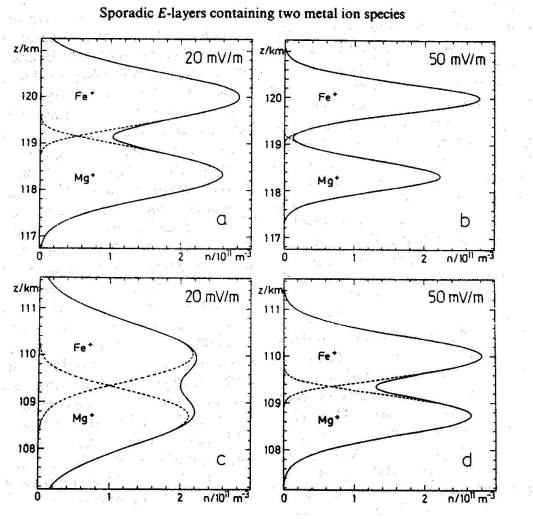


**Figure 7.** Density profile of $Fe^+$ and $Mg^+$ ion layers which accumulate against the pressure gradient in equilibrium as shown in *Nygren et al.* [1984]. The four panels correspond to different electric field direction.

the density profile for $Mg^+$ and $Fe^+$ ions which results when there is a balance between the accumulation of ions and diffusive processes related to the electron and ion pressure gradients [*Nygrén et al.*, 1984a]. Note that the layers readily form over altitudes ranging from 107 to 121 km, and wider ranges are obtained including neutral winds..

### 1.3. Thin Ionization Layers and the Aurora

There seems to be a strong similarity between the thin ionization layers and the enhanced auroral layers. The layers have a similar altitude ranging from 90 to 130 km. The thickness of the layers is similar—ranging from 1 km to several km. Often there are multiple layers which is consistent with multiple ionization layers due to $Fe^+$ and $Mg^+$. The layers both have lifetimes on the order of hours. These similarities provide strong evidence of a connection between the thin ionization layers and the enhanced aurora.

The observations of *Wahlund et al.* [1989] showed simultaneous measurements of electron density obtained from EISCAT radar and a monostatic TV system. Luminosity variations of pulsating aurora were associated with layers in the electron density confirming a connection between luminosity and background density profile. Although *Wahlund et al.* [1989] excluded electric fields as a possible source of the elec-

tron layers because the electric field was not in the correct quadrant, *Bristow and Watkins* [1991]; *Bristow* [1992] and *Bristow and Watkins* [1994] showed that even without a convergent null, thin layers could also accumulate where there is a minimum in flow. The layers were seen to have a large increase in electron temperature while there is a decrease in ion temperature at the electron peak.

## 2. Progress in Understanding Enhanced Aurora

The vertical profile of the enhanced auroral emission cannot be explained by the collisional degradation of an electron beam incident upon the ionosphere as the degradation is primarily due to creation of secondary electrons through neutral collisions and the neutral profiles are not observed to have sharp peaks which could account for enhanced populations of a superthermal electrons as required to produce the observed spectrum [*Hallinan et al.*, 1985, 1997]. Because the enhanced emissions occur mostly uniformly over the spectrum, it is also apparent that they do not result from emissions from an exotic ion species. The most compelling alternative is that the superthermal populations result through a local DC electric field potential drop [*Shepherd and Fälthammar*, 1980] or through wave-particle interactions.

The most obvious source of energy for excitation of plasma waves is the electron beam which produces the auroral ray or its associated currents. In the absence of the aurora there is no emission, therefore, the free energy source for the enhanced emissions is almost certainly the same as the free energy source of the aurora.

### 2.1. Beam Plasma Discharge

The so-called beam plasma discharge has been proposed as a possible source for the enhanced aurora because of similarity with the optical measurements observed during beam plasma discharges in laboratory devices [*Bernstein et al.*, 1978; *Hallinan et al.*, 1988]. In these experiments, an electron beam is driven through a large vacuum chamber which is filled with gas. Below a critical current, the spectrum is dominated by blue glow from $N_2^+1N$ emissions which are caused by excitation of an $N_2$ gas molecule during an ionization collision. When the beam current is increased above a critical value, ignition of the beam-plasma discharge occurs. Such a discharge is characterized by: (1) a large change in geometrical configuration, (2) a large increase in $N_2$ and $N_2^+1N$ emissions, (3) a wave spectrum consisting of significant wave activity with frequency near the plasma frequency, and (4) an increase in electron density and temperature. The increased emissions and electron density occur due to significant ionization. It is of note that initial enhancements are in the $N_2$ emissions just above the threshold and for $N_2^+$ emissions well above the threshold.

Probably the most compelling aspects of this mechanism are that it has an electron beam source, it can heat electrons to form a suprathermal tail, and the emission spectra also seem to have a similarity to the enhanced aurora and the auroral hem spectral measurements. On the other hand, the beam-plasma discharge does not address the following issues: (1) the discharge in the laboratory experiments did not result from a special layer of ambient gas—rather they depended on beam current, so it is likely that the altitude of occurrence of such an enhanced layer would be dependent on the beam energy; however, the enhanced aurora is observed over a wide range of beam energies and the layer remains at roughly fixed altitude in a dynamical aurora, (2) if the discharge disrupts the beam, why does a typical aurora occur below enhanced layers and sharp upper borders?

### 2.2. Ionization Instability

Another suggested mechanism is the so-called ionization instability proposed by *D'Angelo* [1991]. In this instability, ionization gives rise to growing ion-acoustic waves. The basic idea is that the ionization cross section is an increasing function of electron energy. Electrons in the crest of the wave will have higher energy and density and therefore, can produce more ionization in the wave crests leading to wave growth.

Such an instability would be confined to the lower edge of precipitating electrons; therefore, it would not be able to explain enhanced aurora where the curtain extends below the layer. Also, the height of the layer would be determined by the energy of the precipitating electron beam which is inconsistent with layers that are stable on the order of hours. Moreover, such an instability would also be less likely to occur in a heavy ion layer because the ion acoustic speed there (with increased density and mass) would be greatly reduced, and therefore the growth rate would be far less than in the background ionospheric plasma outside of the layers.

### 2.3. Upper Hybrid and Electron Cyclotron Instabilities

Another source of heating of suprathermal electrons is various electrostatic instabilities associated with suprathermal precipitating electrons [*Basu et al.*, 1982; *Chang and Jasperse*, 1992]. Upper hybrid waves can be excited by cyclotron resonance with the suprathermal precipitating electrons or electrostatic electron cyclotron harmonic waves can be excited by the (nonresonant) energetic electrons in thin layers. Quasilinear feedback on the background plasma has been shown to lead to energization of the photoelectrons to energies as high as 6 eV. The instability occurs for altitudes ranging from 100 km to 130 km and it is stabilized below that range by collisional effects and above that range by finite Larmor radius effects. Localization of the instability occurs because unstable harmonics are only excited within narrow altitude layers where the growth rate is maximized. However, the location of the narrow layers depends on the energy distribution of the suprathermal electrons and could be variable during the time scale of auroral precipitation.

## 3. Modified Two-Stream Instability and the Enhanced Aurora

The similarity between the occurrence, location, and vertical extent of thin ionization layers and enhanced aurora suggests that they are related. Moreover, because the location is stationary even during rapid changes in the downcoming electron precipitation and typical aurora are seen below the enhanced layer, it is most likely that there is an instability localized in the thin, heavy metal ionization layers. The fact that multiple layers can be seen also corresponds well with multiple layers due to different ion species. However, as of yet, no theoretical or simulation model has been developed to satisfactorily explain the connection between the ionization layers and the enhancement in the aurora. Because collisional degradation of a precipitating electron beam cannot produce the enhancements, it is likely that a local instability is operating in the thin layer to energize thermal electrons to energies where they can excite the observed $N_2, N_2^+, O_2$ spectral lines. In order to connect the ionization layer with the aurora, the following are necessary requirement of the instability: (a) an increase in suprathermal electron density in the energy range 5-20 eV with a sharp drop off in energy above the ionization energy of $N_2$; (b) the instability must be localized to the thin ionization layer; (c) the instability must be driven by the precipitating electron beam and/or cross-field currents associated with auroral precipitation.

### 3.1. Analytical Theory

Precipitating electrons carry strong field-aligned currents into the ionosphere. In the ionosphere, the current system is closed by cross-field currents carried by ionospheric electrons. Such currents are very effective at generating waves near the lower hybrid frequency [*Krall and Lewer*, 1971; *McBride et al.*, 1972]. A small relative drift (larger than the ion thermal speed) between the ions and electrons across the magnetic field is sufficient to drive the lower hybrid waves unstable.

To illustrate the instability, consider a simple ionospheric plasma model including collisions. Under the influence of a static cross-field electric field the ion and electron fluids have the following velocity response:

$$\mathbf{V} = \left(1 + \frac{\nu_j^2}{\Omega_j^2}\right)^{-1} \nu_j \frac{\mathbf{E}_\perp}{\Omega_j B} + \frac{\mathbf{E} \times \mathbf{B}}{B^2} \qquad (3)$$

At the altitude of interest, $\nu_i, \nu_e \sim 500 - 5000\text{s}^{-1}$ and $\Omega_{ci} \sim 10^2$rad/sec whereas $\Omega_{ce} \sim 10^7$rad/sec so that electrons freely $\mathbf{E} \times \mathbf{B}$ while the ions cannot move effectively across the field on this time scale leading to a zero order velocity $\mathbf{U} = (\mathbf{E} \times \mathbf{B})/B^2$.

Considering electrostatic perturbations we obtain the dispersion relation

$$1 + \frac{k_\perp^2}{k^2}\left(\frac{\omega_{pe}^2}{\Omega_{ce}^2}\frac{(\omega + i\nu_e)}{\omega} - \frac{\omega_{pi}^2}{(\omega - \mathbf{k}\cdot\mathbf{U})(\omega - \mathbf{k}\cdot\mathbf{U} + i\nu_i)}\right) - \frac{k_\parallel^2}{k^2}\frac{\omega_{pe}^2}{\omega(\omega + i\nu_e)} = 0 \qquad (4)$$

Because $\nu_{e,i}/\omega_{pi} \ll 1$ it is appropriate to simplify the dispersion relation by neglecting collisional effects on the timescale of an instability that scales with the ion plasma frequency. The dispersion relation collapses to the well-known dispersion relation for the modified two-stream instability.

$$1 + \frac{k_\perp^2}{k^2}\left(\frac{\omega_{pe}^2}{\Omega_{ce}^2} - \frac{\omega_{pi}^2}{(\omega - \mathbf{k}\cdot\mathbf{U})^2}\right) - \frac{k_\parallel^2}{k^2}\frac{\omega_{pe}^2}{\omega^2} = 0 \qquad (5)$$

In Figure 8 we show the growth rate as a function of $k_\perp U/\omega_{pi}$ based on Equation 5. The growth rate for a thermal plasma [*McBride et al.*, 1972] is similar

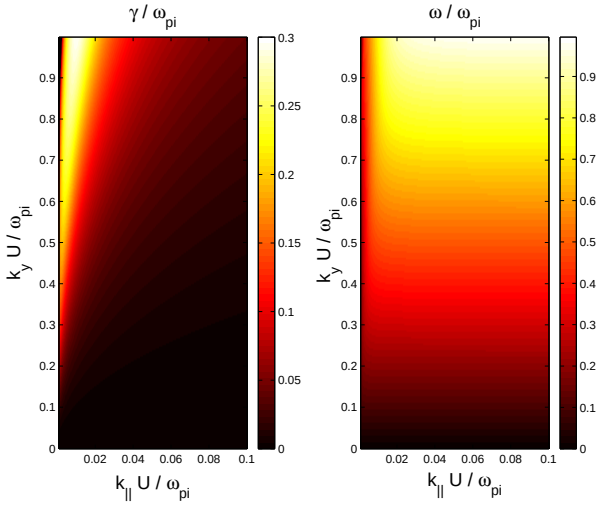


**Figure 8.** Solutions of the dispersion relation defined in Equation 5 for an ion to electron mass ratio of 55200. Shown are a colormap of (a) growth rate, $\gamma$, and (b) real frequency, $\omega$. The dispersion relation only depends on the normalized quantities $\omega/\omega_{pi}$ and $k_\perp U/\omega_{pi}$. The angle of maximum growth is oblique to the magnetic field with $\theta \approx \sqrt{m_e/m_i}$ where $k_\parallel/k_\perp \equiv \tan\theta$ and the maximum growth rate is a fraction of the ion plasma frequency.

with a maximum growth rate around $0.4\omega_{pi}$. In the following table we compare the growth rate in a heavy ion layer with the growth rates outside the layer. Note that the heavy ion densities are 10 times larger than the background $O_2^+$ and $NO^+$ in accordance with observations.

| Species | mass | density ($cm^{-3}$) | $\gamma$ (kHz) |
|---|---|---|---|
| $Fe^+$ | 56 | $10^5$ | 3.4 |
| $Mg^+$ | 24 | $10^5$ | 5.1 |
| $O_2^+$ | 32 | $10^4$ | 1.4 |
| $NO^+$ | 30 | $10^4$ | 1.5 |

It can be seen that the lower hybrid drift instability would grow significantly faster in the thin, dense, heavy metal layers.

### 3.2. Eigenmode Calculation

A relatively simple theoretical calculation illustrates how the growth rate for the lower-hybrid drift instability would be increased in the thin auroral layers. Consider a slab geometry as shown in Figure 9.

For this configuration, there is a background layer of $O_2^+$ or $NO^+$ with thickness $\Lambda$ and a thin metallic ion layer of thickness $\Delta \ll \Lambda$. We solve the differential equation for the wave potential, $\phi$, in the presence of such a thin layer

$$\frac{d^2\phi}{dz^2} = -k_\perp^2 \frac{1+\omega_{pe}^2/\Omega_{ce}^2 - \omega_{pi}^2/(\omega - \mathbf{k}_\perp\cdot\mathbf{U})^2}{1-\omega_{pe}^2/\omega^2} \quad (6)$$

We also impose the boundary condition that $\phi = 0$ at the edge of the plasma. This boundary condition basically discretizes the uniform plasma dispersion relation and becomes more dense (continuous) in the limit that $\Lambda \to \infty$. Because the relative drift is primarily due to electron streaming, the velocity, $\mathbf{U}$ is the same for ions in the ambient plasma as well as the thin metallic layer. For simplicity, we take $\mathbf{k}_\perp$ in the direction of $\mathbf{U}$.

For this calculation, the background layer is assumed to be $NO^+$ with a density of $10^4 cm^{-3}$ and the thin layer is assumed to be either $Mg^+$ or $Fe^+$ with a density of $10^5 cm^{-3}$. The thin layer thickness is $\Delta = 1$km and $\Lambda = 10$km. A magnetic field of 0.5 gauss is assumed. The relative drift velocity $U$ is chosen as the $\mathbf{E}\times\mathbf{B}$ velocity associated with a 1 V/m perpendicular electric field (ions are not able to move with the electrons due to collisions with neutrals).

The eigenfunctions in the slab geometry are sinusoids which obey an eigenvalue condition

$$k_2 \tan(k_1(\Lambda-\Delta)/2) + k_1 \tan(k_2\Delta/2) = 0 \quad (7)$$

for the even modes and

$$k_2 \tan(k_1(\Lambda-\Delta)/2) - k_1 \cot(k_2\Delta/2) = 0 \quad (8)$$

for the odd modes. The wavevectors, $k_1$ and $k_2$ are the solutions of $d^2\phi/dz^2 = k_{1,2}^2\phi$ in the background (1) and thin layer (2) regions respectively. These equations may be solved to provide a discrete spectrum $\omega_j(k_y)$. The solutions in the two regions are sinusoids. In the limit that $\Delta \to 0$, we recover the homogeneous dispersion relation $\omega(k_\parallel, k_\perp)$ in the background region with discrete $k_\parallel = (n+1/2)\pi\Lambda^{-1}$.

In Figure 10 we show the discrete eigenvalues for the background plasma without a thin layer, the odd modes with a thin $Fe^+$ layer, the even modes with a thin $Fe^+$ layer, and the even modes with a thin $Mg^+$ layer. The solutions are shown for $k_\perp U/\omega_{p1} = 0.9$. For that value of the wavevector, the growth rate of the background layer is maximized around $0.35\omega_{p1}^{-1}$. The discrete eigenvalues lie on the arc defined by the local dispersion relation for a homogeneous plasma. The arc shown is not complete as we have omitted the densely packed large $k_\parallel$ modes that have small growth rate. As $\Lambda$ is increased, the density of the modes increases further. The thin, dense, heavy ion

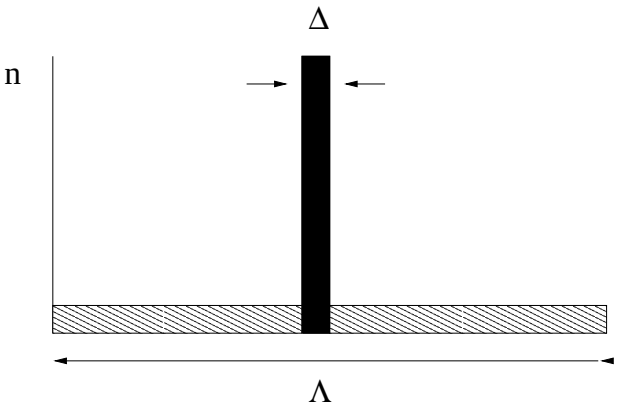


**Figure 9.** Density profile for the eigenmode calculation. A uniform background with density, $n_1$, with an embedded dense, heavy ion layer with density, $n_2$, is assumed. The extent of region 1 is $\Lambda$ and the thickness of the heavy ion layer is $\Delta$.

layer introduces additional modes that are concentrated in the thin layer. Those modes have larger growth rate, and the relative amplitude in the thin layer relative to the outer layer for the fastest growing mode is $10^5$ which means that the fastest growing mode is confined to the thin layer.

This calculation demonstrates that the lower hybrid drift instability can be enhanced in the thin, dense, heavy ion layer. However, it is necessary to perform additional analytical calculations. A study of maximum growth rate should be performed which includes all $k_\perp$. Additional physics should also be included.

Ion and electron thermal effects can be important for stabilizing the mode. If the thin layer and background plasma have the same energy, the higher mass $Fe^+$ ions have a lower thermal velocity, $v_{thi}$. Because the growth rate increases as a function of $(U/v_{thi})$ [*McBride et al.*, 1972] the growth rate would be enhanced in the heavy ion layer. Moreover, electron thermal effects also have a stabilizing effect for larger $k_\parallel$. The maximum growth rate for this instability occurs near $\theta = \tan^{-1}(k_\parallel/k_\perp) \approx \sqrt{m_e/m_i}$, so that the heavy ions drive more oblique modes which suffer less electron Landau damping. In our model calculation, we would expect the background plasma modes with high harmonic number to be suppressed relative to the heavy ion layer modes when thermal effects are included—a possible explanation for why the enhanced aurora is confined to thin layers.

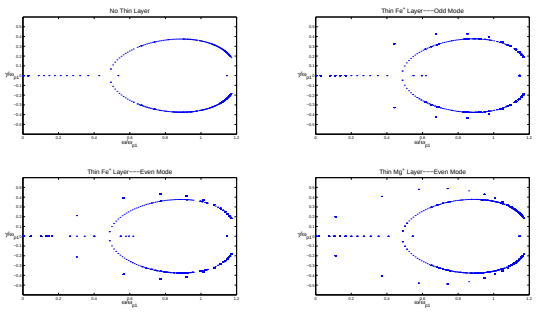


**Figure 10.** Global mode calculations for a slab geometry. In the absence of a thin, dense, heavy ion layer the eigenvalues lie on an arc described by homogeneous plasma theory as shown in the top, left panel. Additional modes appear when there is a thin, dense, heavy ion layer. The growth rate for those modes is enhanced. Kinetic effects could further suppress the instability in the background plasma because ion thermal effects as well as electron Landau damping favor the heavy ion modes that are confined to the thin layers.

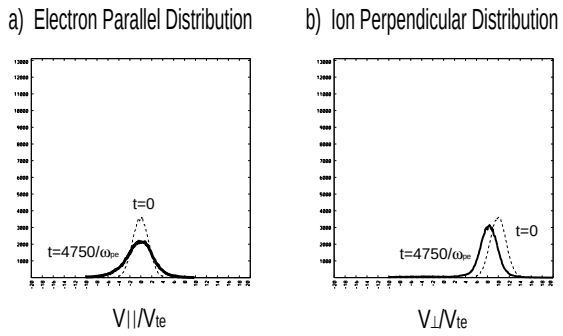


**Figure 11.** A simulation of the $Fe^+$ layer. (a) Electron parallel velocity distribution and (b) ion perpendicular velocity distribution with a mass of 56 $m_{H^+}$ for a simulation of the lower hybrid drift instability which can occur in thin, dense, heavy ion layers in the auroral ionosphere in the presence of cross field currents. The distributions are shown after 4750 $\omega_{pe}$. Note that 1 eV ionospheric electrons are strongly heated in the field-aligned direction forming an energetic tail with energies in the range 10-100 eV. Heavy ions are slowed reducing the cross field current. The energetic electrons have sufficient energy to ionize $N_2^+$ molecules as required to explain enhanced aurora with emission from the $N_2^+$ ionized state.

### 3.2.1. Simulation Model for the Thin Auroral Layer

In order to study the effect of the lower hybrid drift instability on electron heating, we used a 2 1/2D electrostatic particle code appropriate for low frequency waves in a plasma in a strong magnetic field [*Okuda and Lee*, 1978]. In the simulation model, electrons are treated as guiding center particles whereas the full ion dynamics are followed in time which is justified in this case where the frequency of the lower hybrid drift waves lies between the electron and ion gyro-frequencies.

A simulation was performed for an $Fe^+$ heavy ion layer ($m_i/m_e = 102,827$) where the $Fe^+$ ions are drifting across the electrons at 10 times the ion thermal speed. Such a relative drift is easily attained for an auroral electric field of 1 V/m. Since the relative drift is much less than the electron thermal speed, 0.031, no electron cyclotron instabilities are expected justifying the use of the electron drift approximation. Shown in Figure 11 are the electron velocity distribution along magnetic field (a) and the $Fe^+$ perpendicular velocity distribution (b) at t = 0 and $4750/\omega_{pe}^{-1}$. Note the electrons are heated more or less symmetrically while the $Fe^+$ ions have slowed down while at the same time heated slightly. The high energy tail of the electrons has reached 5-10 times the thermal speed so that the energy of these electrons can reach 2-40 eV if the initial thermal electron energy is about 0.4 eV. These electrons should be able to excite and ionize background nitrogen molecules. Therefore the instability can explain enhanced light emission observed in the auroral ionosphere. While the simulation model used is a one-species ion model, preliminary simulations with a heavy ion density peak embedded in the ionospheric plasma have shown excitation of strong lower hybrid instabilities in the heavy ion layer.

## 4. Summary

The luminosity in visible auroral forms is typically distributed vertically over an altitude range of several tens to hundreds of kilometers. The luminosity profiles normally agree well with calculated profiles for the collisional ionization and excitation by atmospheric particles by precipitating electrons having energies 100eV-10keV. However, auroras frequently (typically more than 50% of the time) exhibit enhanced intensity within relatively thin horizontal layers.

These layers appear to be relatively stable atmospheric structures and may be observed near the same altitude over several hours—even in the presence of auroras with high variability. Radar observations also show enhancements in the background electron density around the same altitude. The electron enhancement is apparently related to an accumulation of heavy $Fe^+$ and $Mg^+$ into thin layers which occurs for specific orientations of the ionospheric electric field. The similarity in altitude and duration of the enhanced aurora and heavy ion layers suggests a connection. It is also apparent from the spectral data that the enhanced luminosity is the result of energization of thermal ionospheric electrons which most likely results from wave-particle interaction.

Our objective is to provide a theoretical connection between thin ionization layers in the E-region of the ionosphere and the enhanced aurora. To establish this connection we performed analytical studies of wave instabilities for a thin, dense, heavy ion layer in the presence of energetic precipitating electrons and associated cross-field ionospheric currents. These studies are complimented by 2-1/2D and particle simulations of electrostatic plasma instabilities that would occur in the thin ionization layers. The simulations demonstrate that significant heating occurs that could produce an energetic electron tail in the distribution of the ambient electron population with sufficient energy to produce the observed 4278Å $N_2^+$ emission band.

**Acknowledgments** This work was supported by NASA Grant NAG5-10971, NSF Grant ATM-9819705, NASA Grant W-19880, NSF Grant ATM-0411392, and DoE Contract No. DE-AC02-76-CHO-3073.

## References

Axford, W. I., The formation and vertical movement of dense ionized layers in the ionosphere due to neutral wind shear, *J. Geophys. Res.*, *68*, 769–779, 1963.

Basu, B., T. Chang, and J. R. Jasperse, Electrostatic plasma instabilities in the daytime lower ionosphere, *Geophys. Res. Lett.*, *9*, 68–71, 1982.

Behnke, R. A., and J. F. Vickrey, Radar evidence for $Fe^+$ in a sporadic-E layer, *Radio Sci.*, *10*, 325–327, 1975.

Bernstein, W., et al., Electron beam injection experiments: The beam-plasma discharge at low pres-

sures and magnetic field strengths, *Geophys. Res. Lett.*, *5*, 127–130, 1978.

Bristow, W. A., The formation and characteristics of E-region thin ionization layers at high latitudes, Ph.D. thesis, University of Alaska, Fairbanks, 1992.

Bristow, W. A., and B. J. Watkins, Numerical simulation of the formation of thin ionization layers at high latitudes, *Geoph. Res. Lett.*, *18*(3), 404–407, 1991.

Bristow, W. A., and B. J. Watkins, Incoherent-scatter observations of thin ionization layers at Sondrestrom, *J. Atmosph. Terr. Phys.*, *55*(6), 873–894, 1993.

Bristow, W. A., and B. J. Watkins, Effects of the large-scale convection electric field structure on the formation of thin ionization layers at high latitudes, *J. Atmosph. Terr. Phys.*, *56*(3), 401–415, 1994.

Chang, T., and J. R. Jasperse (eds.), *Theory and Observations of High Frequency Electrostatic Plasma Instabilities in the Lower Ionosphere*, no. 12 in Physics of Space Plasmas (1992), Cambridge, MA. Scientific Publishers, Inc., Proceedings of the 1992 Cambridge Workshop in Geoplasma Physics, 1992.

D'Angelo, N., On the Stenbaek-Neilsen and Hallinan pulsating auroras, *J. Geophys. Res.*, *96*, 1831–1832, 1991.

Dungey, J. W., Effect of a magnetic field on turbulence in an ionized gas, *J. Geophys. Res.*, *64*, 2188–2191, 1963.

Hallinan, T. J., H. C. Stenbaek-Nielsen, and C. S. Deehr, Enhanced aurora, *J. Geophys. Res.*, *90*, 8461–8475, 1985.

Hallinan, T. J., C. S. Deehr, E. Hoch, R. Viereck, W. Bernstein, and A. Konradi, Spectral signature of the beam plasma discharge, *J. Geophys. Res.*, *93*, 7586–7590, 1988.

Hallinan, T. J., J. Kimball, H. C. Stenbaek-Nielsen, and C. S. Deehr, Spectroscopic evidence for suprathermal electrons in enhanced auroras, *J. Geophys. Res.*, *102*, 7501–7508, 1997.

Hallinan, T. J., J. Kimball, D. Osborne, and C. S. Deehr, Spectra of type-B red lower borders, *J. Geophys. Res.*, *103*, 11,635–11,640, 1998.

Kelley, M. C., *The Earth's Ionosphere*. Academic Press, p 233, 1989.

Krall, N. A., and P. C. Lewer, Low-frequency instabilities in magnetic pulses, *Phys. Rev. A*, *4*, 2094–2103, 1971.

Nygrén, T., L. Jalonen, and A. Huuskonen, Density profiles of sporadic E-layers containing two metal ion species, *J. Atmos. Terr. Phys.*, *46*, 885–893, 1984a.

Nygrén, T., L. Jalonen, J. Oskman, and T. Turunen, The role of electric field and neutral wind direction in the formation of sporadic e-layers, *J. Atmos. Terr. Phys.*, *46*, 373–381, 1984b.

McBride, J. B., E. Ott, J. P. Boris, and J. H. Orens, Theory and simulation of turbulent heating by the modified two-stream instability, *Phys. Fluids*, *15*, 2367–2379, 1972.

Narcisi, R. S., A. D. Bailey, and L. Della Lucca, Composition measurements of sporadic-E in the night time lower ionosphere, *Space Res.*, *7*, 123, 1968.

Okuda, H., and W. Lee, A simulation model for studying low frequency microinstabilities, *J. Comput. Phys.*, *26*, 139–152, 1978.

Shepherd, G. E., and C.-G. Fälthammar, Implications of extreme thinness of pulsating auroral structures, *J. Geophys. Res.*, *85*, 217–218, 1980.

Störmer, C., *The Polar Aurora*. Oxford University Press, New York, 1955.

Turunen, T., T. Nygren, A. Huskonen, and L. Jalonen, Incoherent scatter studies of sporadic-E using 300m resolution, *J. Atmosph. Terr. Phys.*, *50*, 277–287, 1988.

Wahlund, J.-E., H. J. Opgenoorth, and P. Rothwell, Observations of thin auroral ionization layers by EISCAT in connection with pulsating aurora, *J. Geophys. Res.*, *94*, 17,223–17,233, 1989.

Whitehead, J. D., The formation of the sporadic e-layer in the temperate zones, *J. Atmos. Terr. Phys.*, *20*, 49–58, 1961.

This preprint was prepared with the AGU LaTeX macros v3.0. File enhanced formatted 2008 May 12.

With the extension package 'AGU$^{++}$', version 1.2 from 1995/01/12

The Princeton Plasma Physics Laboratory is operated
by Princeton University under contract
with the U.S. Department of Energy.

Information Services
Princeton Plasma Physics Laboratory
P.O. Box 451
Princeton, NJ 08543

Phone: 609-243-2750
Fax: 609-243-2751
e-mail: pppl_info@pppl.gov
Internet Address: http://www.pppl.gov